

Synthesis and Properties of Palladium Diselenolenes: X-ray Crystal Structures of $[\text{Pd}\{\text{SeC}(\text{R}^1)=\text{C}(\text{R}^2)\text{Se}\}(\text{PBU}_3)_2]$ [$\text{R}^1, \text{R}^2 = (\text{CH}_2)_n$, $n = 4, 5, 6$]

Susan Ford,[†] Christopher P. Morley,^{*†} and Massimo Di Vaira[‡]

Department of Chemistry, University of Wales Swansea, Singleton Park, Swansea, U.K. SA2 8PP, and Dipartimento di Chimica, Università degli studi di Firenze, Via della Lastruccia 3, 50019 Sesto Fiorentino (FI), Italy

Received May 12, 2004

The reaction between $[\text{Pd}_2(\text{dba})_3]$ (dba = dibenzylideneacetone), tributylphosphine, and a bis(cycloalkeno)-1,4-diselenin leads to either a mononuclear diselenolene $[\text{Pd}\{\text{SeC}(\text{R}^1)=\text{C}(\text{R}^2)\text{Se}\}(\text{PBU}_3)_2]$ or a dinuclear diselenolene $[\text{Pd}_2\{\text{SeC}(\text{R}^1)=\text{C}(\text{R}^2)\text{Se}\}_2(\text{PBU}_3)_2]$ [$\text{R}^1, \text{R}^2 = (\text{CH}_2)_n$, $n = 4, 5, 6$] depending on the stoichiometry employed. Treatment of the dinuclear diselenolenes with 1,2-bis(diphenylphosphino)ethane (dppe) provides a high-yielding route to the mononuclear species $[\text{Pd}\{\text{SeC}(\text{R}^1)=\text{C}(\text{R}^2)\text{Se}\}(\text{dppe})]$. All new compounds have been characterized by standard spectroscopic and analytical techniques, in particular by multinuclear NMR spectroscopy; the structure of each of the mononuclear tributylphosphine complexes has been determined by X-ray crystallography. Computational studies show that the observed asymmetry of the diselenolenes in the solid state is a result primarily of intramolecular repulsive interactions between the ligands.

Introduction

For many years, the potentially useful electrochemical and optical properties of transition metal dithiolenes have attracted the attention of chemists, physicists, and materials scientists.¹ Possible areas of application include molecular electronics, infrared dyes, liquid crystals, and catalysis.^{2–4} By contrast, the selenium analogues of dithiolenes (diselenolenes) have been little studied,^{5–10} largely because of the lack of generally applicable preparative methods. These complexes are, however, attractive synthetic targets as the incorporation of selenium should lead to a smaller HOMO–

LUMO gap and an increase in the strength of intermolecular interactions in the solid state.

The reactions of 1,2,3-selenadiazoles with low-valent transition metal compounds have previously been used, by us¹¹ and others,¹² to prepare a wide variety of selenium-

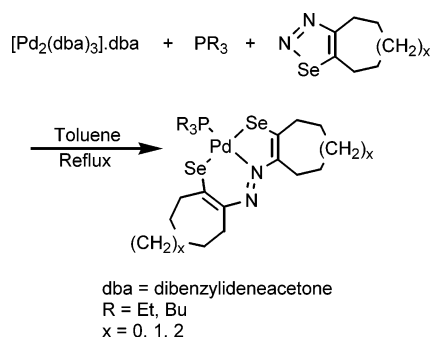
* To whom correspondence should be addressed. E-mail: c.p.morley@swan.ac.uk.

[†] University of Wales Swansea.

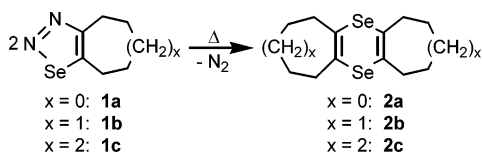
[‡] Università degli studi di Firenze.

- (1) (a) Karlin, K. D.; Stiefel, E. I., Eds. *Dithiolene Chemistry: Synthesis, Properties, and Applications*; Progress in Inorganic Chemistry Series; Wiley: New York, 2004; Vol. 52. (b) Müller-Westerhoff, U. T.; Vance, B. In *Comprehensive Coordination Chemistry*; Wilkinson G., Ed.; Pergamon Press: Oxford, U.K., 1988; Vol. 2, Chapter 16.5, p 595.
- (2) Cassoux, P.; Valade, L.; Kobayashi, H.; Clark, R. A.; Underhill, A. E. *Coord. Chem. Rev.* **1991**, *110*, 115.
- (3) Bjørnholm, T.; Geisler, T.; Petersen, J. C.; Grieve, D. R.; Schjødt, N. C. *Non-Linear Optics* **1995**, *10*, 129.
- (4) Coomber, A. T.; Beljonne, D.; Friend, R. H.; Brédas, J. L.; Charlton, A.; Robertson, N.; Underhill, A. E.; Kurmoo, M.; Day, P. *Nature* **1996**, *380*, 144.
- (5) (a) Sandman, D. J.; Stark, J. C.; Allen, G. W.; Acampora, L. A.; Jansen, S.; Jones, M. T.; Ashwell, G. J.; Foxman, B. M. *Inorg. Chem.* **1987**, *26*, 1664. (b) Gautheron, B.; Tainturier, G.; Pouly, S.; Theobald, F.; Vivier, H.; Laarif, A. *Organometallics* **1984**, *3*, 1495. (c) Klapötke, T. M. *Phosphorus, Sulfur, Silicon* **1989**, *41*, 105.
- (6) (a) Papavassiliou, G. C. *Mol. Cryst. Liq. Cryst.* **1982**, *86*, 159. (b) Matsubayashi, G.; Yokazawa, A. *J. Chem. Soc., Dalton Trans.* **1990**, 3535. (c) Faulmann, C. Legros, J.-P.; Cassoux, P.; Cornelissen, J.; Brossard, L.; Inokuchi, M.; Tajima, H.; Tokumoto, M. *J. Chem. Soc., Dalton Trans.* **1994**, 249. (d) Zeltner, S.; Olk, R. M.; Pink, M.; Jelonek, S.; Jorchel, P.; Gelbrich, T.; Sieler, J.; Kirmse, R. *Z. Anorg. Allg. Chem.* **1996**, *622*, 1979.
- (7) (a) Heuer, W. B.; Squattrito, P. J.; Hoffman, B. M.; Ibers, J. A. *J. Am. Chem. Soc.* **1988**, *110*, 792. (b) Wudl, F.; Zellers, E. T.; Cox, S. D. *Inorg. Chem.* **1985**, *24*, 2864.
- (8) Bollinger, C. M.; Rauchfuss, T. B. *Inorg. Chem.* **1982**, *21*, 3947.
- (9) (a) Okano, Y.; Sawa, H.; Aonuma, S.; Kato, R. *Chem. Lett.* **1993**, 1851. (b) McCullough, R. D.; Belot, J. A.; Seth, J.; Rheingold, A. L.; Yap, G. P. A.; Cowan, D. O. *J. Mater. Chem.* **1995**, *5*, 1581.
- (10) (a) Kajitani, M.; Ochiai, R.; Dohki, K.; Kobayashi, N.; Akiyama, T.; Sugimori, A. *Bull. Chem. Soc. Jpn.* **1989**, *62*, 3266. (b) Miller, E. J.; Landon, S. J.; Brill, T. B. *Organometallics* **1985**, *4*, 533.
- (11) (a) Morley, C. P. *Organometallics* **1989**, *8*, 800. (b) Dorrity, M. R. J.; Lavery, A.; Malone, J. F.; Morley, C. P.; Vaughan, R. R. *Heteroatom Chem.* **1992**, *3*, 87. (c) Morley, C. P.; Vaughan, R. R. *J. Organomet. Chem.* **1993**, *444*, 219.

Scheme 1



Scheme 2



containing complexes. In particular, we have shown that cyclopentadienylcobalt diselenolenes can be produced by this route.¹³

We recently extended this methodology to the synthesis of dinuclear diselenolenes based on the triphenylphosphine-palladium fragment, starting from the palladium(0) complex [Pd(PPh₃)₃].¹⁴ The reactions of trialkylphosphinepalladium(0) precursors with cycloalkeno-1,2,3-selenadiazoles proceed via a different route to give the azo complexes shown in Scheme 1.¹⁵

Despite their ready preparation from 1,2,3-selenadiazoles¹⁶ (Scheme 2), little research into the chemistry of 1,4-diselenins has been documented.^{17–19} We have now examined the reactions of bis(cycloalkeno)-1,4-diselenins with a tributylphosphinepalladium(0) complex, and in this paper, we present the results of our study. A preliminary report of some of this work has already been published.²⁰

Experimental Section

All reactions were performed using standard Schlenk techniques and predried solvents under an atmosphere of dinitrogen. ¹H and ¹³C NMR spectra were obtained on a Bruker AC400 instrument using tetramethylsilane as an internal standard. ³¹P and ⁷⁷Se NMR spectra were obtained on a Bruker WM250 instrument using 85%

phosphoric acid or dimethyl selenide as an external standard. UV/Vis spectra were obtained on a Perkin-Elmer Lambda 9 instrument. Mass spectra were recorded by the EPSRC Mass Spectrometry Centre using fast atom bombardment (FAB).

Cycloalkeno-1,2,3-selenadiazoles **1a–c**,¹⁶ bis(cycloalkeno)-1,4-diselenins **2a–c**,¹⁶ and [Pd₂(dba)₃]·dba²¹ were prepared by literature methods. Tributylphosphine, triethylphosphine, and 1,2-bis(diphenylphosphino)ethane (dppe) were obtained commercially (Aldrich) and used without further purification.

Synthesis of Tributylphosphine-Palladium Diselenolenes (3a–c, 4a–c, and 5a). (a) **3a, 4a, and 5a.** PBu₃ (0.16 g, 0.80 mmol) was added to a xylene solution (100 cm³) of [Pd₂(dba)₃]·dba (0.23 g, 0.20 mmol). After the mixture had been stirred at room temperature for a short time, bis(cyclohexeno)-1,4-diselenin, **2a** (0.14 g, 0.44 mmol), was added, and the mixture was heated to reflux overnight. Removal of the solvent under reduced pressure left a dark colored oil, which was purified by column chromatography on an alumina column with toluene as the eluent. Collection of the deep purple band and recrystallization from hexane gave **3a** as an analytically pure solid. Yield: 0.05 g.

Use of one-half of the above quantity of PBu₃ gave the analogous dinuclear compound **4a** by an identical procedure. In addition, in this case, a second band was eluted from the chromatography column using toluene/diethyl ether (5:1). Removal of the solvent under reduced pressure left a deep red oil, which was recrystallized from hexane to give **5a** as an analytically pure solid. Yield: 0.04 g.

(b) **3b,c and 4b,c.** In a typical experiment, PBu₃ (0.16 g, 0.80 mmol) was added to a toluene solution (100 cm³) of [Pd₂(dba)₃]·dba (0.23 g, 0.20 mmol). After the mixture had been stirred at room temperature for a short time, bis(cyclohepteno)-1,4-diselenin, **2b** (0.15 g, 0.43 mmol), was added, and the mixture was heated to reflux for 1 h. Removal of the solvent under reduced pressure left a dark colored oil, which was purified by column chromatography on an alumina column with toluene as the eluent. Collection of the deep purple band and recrystallization from hexane gave **3b** as an analytically pure solid. Yield: 0.05 g.

Use of one-half of the above quantity of PBu₃ gave the analogous dinuclear compound **4b** by an identical procedure. Compounds **3c** and **4c** were prepared similarly from **2c**. Yields and spectroscopic and analytical data for **3a–c**, **4a–c**, and **5a** are summarized in Tables 1–4.

Conversion of 4a–c to 3a–c. In a typical experiment, PBu₃ (0.08 g, 0.40 mmol) was added to a toluene solution (50 cm³) of **4a** (0.11 g, 0.10 mmol). The mixture was stirred at room temperature for 1 h. Removal of the solvent under reduced pressure left a dark colored oil, which was purified by column chromatography on an alumina column with toluene as the eluent. Collection of the deep purple band and recrystallization from hexane gave **3a** as an analytically pure solid. Yield: 0.11 g.

Reaction of 4a–c with PET₃. In a typical experiment, PET₃ (0.08 g, 0.68 mmol) was added to a toluene solution (50 cm³) of **4a** (0.11 g, 0.10 mmol). The mixture was stirred at room temperature for 1 h. After this time, the ³¹P NMR spectrum of an aliquot contained three singlets, two of which corresponded to PET₃ (δ = –19.2 ppm) and PBu₃ (δ = –31.7 ppm). The third resonance (δ = 8.8 ppm) was assigned to the product [Pd(Se₂C₆H₈)(PET₃)₂]. Removal of the solvent under reduced pressure left a dark colored oil, which was purified by column chromatography on an alumina column with toluene/ethyl acetate (4:1) as the eluent. Collection of the deep

- (12) (a) Gilchrist, T. L.; Mente, P. G.; Rees, C. W. *J. Chem. Soc., Perkin Trans. 1* **1972**, 2165. (b) Schrauzer, G. N.; Kisch, H. *J. Am. Chem. Soc.* **1973**, 95, 2501. (c) Pannell, K. H.; Mayr, A. J.; Hoggar, R.; Pettersen, R. C. *Angew. Chem., Int. Ed. Engl.* **1980**, 19, 632. (d) Bätzel, V.; Böse, R. Z. *Naturforsch. B* **1981**, 38, 172.
- (13) Morley, C. P.; Vaughan, R. R. *J. Chem. Soc., Dalton Trans.* **1993**, 703.
- (14) Ford, S.; Khanna, P. K.; Morley, C. P.; Di Vaira, M. *J. Chem. Soc., Dalton Trans.* **1999**, 791.
- (15) Ford, S.; Morley, C. P.; Di Vaira, M. *J. Chem. Soc., Chem. Commun.* **1998**, 1305.
- (16) Meier, H.; Voigt, E. *Tetrahedron* **1972**, 28, 187.
- (17) Bates, C. M.; Khanna, P. K.; Morley, C. P.; Di Vaira, M. *J. Chem. Soc., Chem. Commun.* **1997**, 913.
- (18) (a) Dorrity, M. R. J.; Lavery, A.; Malone, J. F.; Morley, C. P.; Vaughan, R. R. *Heteroatom Chem.* **1992**, 3, 87. (b) Chesney, A.; Bryce, M. R.; Batsanov, A. S.; Howard, J. A. K. *J. Chem. Soc., Chem. Commun.* **1997**, 2293.
- (19) Mayr, A. J.; Lien, H.-S.; Pannell, K. H.; Parkanyi, L. *Organometallics* **1985**, 4, 1580.
- (20) Ford, S.; Morley, C. P.; Di Vaira, M. *New J. Chem.* **1999**, 23, 811.

- (21) Takahashi, Y.; Ito, T.; Sakai, S.; Ishii, Y. *J. Chem. Soc., Chem. Commun.* **1970**, 1065.

Table 1. ^1H NMR Spectroscopic Data for **3a–c**, **4a–c**, and **5a** in CDCl_3 Solution

	3a	3b	3c	4a	4b	4c	5a
CH_3	0.92 (t) ^a	0.92 (t) ^a	0.92 (t) ^a	0.92 (t) ^a	0.92 (t) ^a	0.92 (t) ^a	0.92 (t) ^a
	—	—	—	—	—	—	0.97 (t) ^b
CH_2P	1.84 (m)	1.80 (m)	1.83 (m)	1.45–1.75	1.47–1.72	1.43–1.81	1.63 (m)
	—	—	—	—	—	—	1.75 (m)
$\text{CH}_2\text{CH}_2\text{P}$	1.48 (m)	1.47 (m)	1.48 (m)	1.45–1.75	1.47–1.72	1.43–1.81	1.26–1.57
$\text{CH}_3\text{CH}_2\text{CH}_2$	1.42 (m)	1.41 (m)	1.42 (m)	1.41 (m)	1.41 (m)	1.38 (m)	1.26–1.57
$\gamma\text{-CH}_2$	—	1.47 (m)	1.48 (m)	—	1.47–1.72	1.43–1.81	—
$\beta\text{-CH}_2$	1.64 (m)	1.63 (m)	1.63 (m)	1.45–1.75	1.47–1.72	1.43–1.81	1.97 (m, 2H)
	—	—	—	—	—	—	2.26 (m, 2H)
	—	—	—	—	—	—	2.48 (m, 4H)
$\alpha\text{-CH}_2$	2.50 (m)	2.54 (m)	2.53 (m)	2.38–2.64	2.41–2.65	2.36–2.75	2.53–2.82

^a $^3J(\text{H}^1\text{H}^1\text{H}) = 7.1$ Hz. ^b $^3J(\text{H}^1\text{H}^1\text{H}) = 6.8$ Hz.

Table 2. ^{13}C NMR Spectroscopic Data for **3a–c**, **4a–c**, and **5a** in CDCl_3 Solution

	3a	3b	3c	4a	4b	4c	5a
CH_3	13.8	13.7	13.7	13.8	13.8	13.8	13.6, 13.9
CH_2P	25.2 ^a	24.9 ^a	25.1 ^a	24.3 ^d	24.3 ^d	24.2 ^d	21.4, ^f 24.2 ^g
$\text{CH}_2\text{CH}_2\text{P}$	24.4 ^b	24.4 ^b	24.4 ^b	24.4 ^e	24.4 ^e	24.4 ^e	24.1, ^e 24.4 ^h
$\text{CH}_3\text{CH}_2\text{CH}_2$	26.3	26.2	26.2	26.4	26.5	26.4	26.4
$\text{C}=\text{C}$	127.5 ^c	131.4 ^c	130.1 ^c	117.4	120.7	119.6	116.7, 120.0
	—	—	—	145.1	151.0	149.7	140.2, 146.8
$\alpha\text{-CH}_2$	35.1	39.9	37.3	36.1	40.6	37.3	35.9, 37.2
	—	—	—	38.1	43.6	40.2	38.6, 40.6 ⁱ
$\beta\text{-CH}_2$	22.6	29.7	30.8	22.3	30.9	30.8	22.8, ^j 23.2
	—	—	—	23.4	33.1	30.8	30.5, 30.7
$\gamma\text{-CH}_2$	—	27.3	26.4	—	27.3	26.0	—
	—	—	—	—	—	26.4	—

^a Apparent triplet: average $J(^{13}\text{C}-^{31}\text{P}) = 7$ Hz (**3a**, **3b**), 6 Hz (**3c**).

^b Apparent triplet: average $J(^{13}\text{C}-^{31}\text{P}) = 13$ Hz (**3a**), 12 Hz (**3b**, **3c**).

^c Apparent triplet: average $J(^{13}\text{C}-^{31}\text{P}) = 7$ Hz (**3a**, **3b**), 6 Hz (**3c**).

^d $^1J(^{13}\text{C}-^{31}\text{P}) = 25$ Hz (**4a**, **4c**), 21 Hz (**4b**). ^e $^2J(^{13}\text{C}-^{31}\text{P}) = 14$ Hz.

^f $^1J(^{13}\text{C}-^{31}\text{P}) = 51$ Hz. ^g $^1J(^{13}\text{C}-^{31}\text{P}) = 50$ Hz. ^h $^2J(^{13}\text{C}-^{31}\text{P}) = 16$ Hz.

ⁱ $^4J(^{13}\text{C}-^{31}\text{P}) = 23$ Hz. ^j $^5J(^{13}\text{C}-^{31}\text{P}) = 5$ Hz.

Table 3. ^{31}P and ^{77}Se NMR Spectroscopic Data for **3a–c**, **4a–c**, and **5a** in CDCl_3 Solution

	3a	3b	3c	4a	4b	4c	5a
^{31}P	1.4 ^a	0.8 ^a	0.7 ^a	10.9	11.2	9.6	19.8, 8.9
^{77}Se	512 ^b	533 ^b	519 ^b	472	498	493	not observed
	—	—	—	410 ^c	434 ^c	407 ^c	418, 391

^a $^2J(^{31}\text{P}-^{31}\text{P}) = 44$ Hz. ^b $^2J(^{77}\text{Se}-^{31}\text{P}_{\text{trans}}) = 65$ Hz (**3a**, **3b**), 67 Hz (**3c**); $^2J(^{77}\text{Se}-^{31}\text{P}_{\text{cis}}) = 16$ Hz (**3a–c**). ^c $^2J(^{77}\text{Se}-^{31}\text{P}_{\text{trans}}) = 111$ Hz (**4a**, **4c**), 110 Hz (**4b**); $^2J(^{77}\text{Se}-^{31}\text{P}_{\text{cis}}) = 9$ Hz (**4a–c**).

purple band gave an oily solid whose mass spectrum contained peaks due to **3a**, **4a**, $[\text{Pd}(\text{Se}_2\text{C}_6\text{H}_8)(\text{PET}_3)(\text{PBU}_3)]$ ($m/e = 666$), and $[\text{Pd}_2(\text{Se}_2\text{C}_6\text{H}_8)_2(\text{PET}_3)(\text{PBU}_3)]$ ($m/e = 1012$).

Synthesis of dppe-Palladium Diselenolenes (6a–c). (a) **From 1,2,3-Selenadiazoles 1a–c or 1,4-Diselenins 2a–c.** In a typical experiment, dppe (0.16 g, 0.40 mmol) was added to a toluene solution (100 cm^3) of $[\text{Pd}_2(\text{dba})_3]\cdot\text{dba}$ (0.23 g, 0.20 mmol). After the mixture had been stirred at room temperature for a short time, cyclohexeno-1,2,3-selenadiazole, **1a** (0.16 g, 0.86 mmol), or bis-(cyclohexeno)-1,4-diselenin, **2a** (0.14 g, 0.44 mmol), was added,

and the mixture was heated to reflux for 1 h. Removal of the solvent under reduced pressure left an orange oil, which was purified by column chromatography on an alumina column. Two yellow bands were initially obtained with toluene as the eluent. Collection of the brown third band using a mixture of toluene and ethyl acetate (4:1) and recrystallization from toluene gave **6a** as an analytically pure, pink solid. Yield: 0.02 g.

(b) **From 4a–c.** In a typical experiment, dppe (0.08 g, 0.20 mmol) was added to a toluene solution (50 cm^3) of **4a** (0.11 g, 0.10 mmol). The mixture was stirred at room temperature for 1 h. Concentration of the solution by removal of the solvent under reduced pressure resulted in the precipitation of **6a** as a pink solid, which was collected by filtration and recrystallized from toluene. Yield: 0.10 g.

Yields and spectroscopic and analytical data for **6a–c** are summarized in Tables 5–8.

X-ray Crystallography. Details of the crystal structure determinations are presented in Table 9. Data for **3b** have been reported previously, as part of a preliminary communication,²⁰ and are included here for comparison purposes. Measurements were carried out at room temperature with an Enraf-Nonius CAD4 diffractometer for **3a** and **3b**, using graphite-monochromated Mo $\text{K}\alpha$ radiation, and with a Siemens-Bruker P4 diffractometer mounted on a rotating anode generator for **3c**, using graphite-monochromated Cu $\text{K}\alpha$ radiation. Empirical corrections for absorption were applied, based on ψ scans. Structure solution was by direct methods with SIR97²² and Fourier cycles with SHELXL-93,²³ which was also used for structure refinements. The final refinement cycles were performed against F^2 with all non-hydrogen atoms anisotropic and hydrogen atoms in calculated positions. Drawings were made with ORTEP.²⁴ Crystallographic data (excluding structure factors) for the structures reported in this paper have been deposited with the Cambridge Crystallographic Data Centre as supplementary publication nos. CCDC 250883 (**3a**), CCDC 440/126 (**3b**), and CCDC 250882 (**3c**). Copies of the data can be obtained free of charge on application to CCDC, 12 Union Road, Cambridge CB2 1EZ, U.K. [Fax: int. code +44 (0)1223 336033; e-mail: deposit@ccdc.cam.ac.uk].

Computation. Conformational searches, in some cases with constraints described in the Results and Discussion section, were

Table 4. Yields, Melting Points, and Mass Spectrometric Data for **3a–c**, **4a–c**, and **5a**

	3a	3b	3c	4a	4b	4c	5a
yield (%)	17 ^b	14 ^b	11 ^b	15	14	54	18
melting point ($^\circ\text{C}$)	99	119	114	— ^c	— ^c	112–113	118–119
mass spectrometric data ^a							
M^+	750 (100%)	764 (60%)	778 (100%)	1096 (100%)	1124 (100%)	1148 (100%)	1176 (100%)
$[\text{M}-\text{PBU}_3]^+$	548 (73%)	562 (100%)	576 (30%)	894 (31%)	922 (82%)	946 (71%)	—

^a Recorded using FAB; figures are for isotopomers containing ^{80}Se , ^{106}Pd . ^b Isolated yields from **4a–c**: ~75%. ^c Compounds not obtained in crystalline form.

Table 5. ^1H NMR Spectroscopic Data for **6a–c** in CDCl_3 Solution

	6a	6b	6c
CH_2P	2.37 (m) ^a	2.35 (m) ^a	2.35 (m) ^a
<i>o</i> - C_6H_5	7.36 (m)	7.36 (m)	7.35 (m)
<i>m</i> - C_6H_5	7.72 (m)	7.71 (m)	7.70 (m)
<i>p</i> - C_6H_5	7.15 (m)	7.16 (m)	7.14 (m)
γ - CH_2	—	1.34 (m)	1.34 (m)
β - CH_2	1.57 (m)	1.51 (m)	1.53 (m)
α - CH_2	2.45 (m)	2.50 (m)	2.51 (m)

^a Apparent doublet: average $J(^1\text{H}-^{31}\text{P}) = 10.3$ Hz (**6a**), 10.2 Hz (**6b**, **6c**).

Table 6. ^{13}C NMR Spectroscopic Data for **6a–c** in CDCl_3 Solution

	6a	6b	6c
CH_2P	28.7 ^a	28.3 ^a	28.0 ^a
<i>o</i> - C_6H_5	133.4 ^b	133.3 ^b	133.3 ^b
<i>m</i> - C_6H_5	128.8 ^c	128.8 ^c	128.8 ^c
<i>p</i> - C_6H_5	131.2	131.1	131.1
<i>ipso</i> - C_6H_5	130.5 ^d	130.8 ^d	130.7 ^d
$\text{C}=\text{C}$	129.6 ^e	132.6 ^e	131.4 ^e
α - CH_2	35.7	40.3	37.7
β - CH_2	22.7	29.7	30.7
γ - CH_2	—	27.2	26.5

^a Apparent triplet: average $J(^{13}\text{C}-^{31}\text{P}) = 24$ Hz. ^b Apparent triplet: average $J(^{13}\text{C}-^{31}\text{P}) = 6$ Hz. ^c Apparent triplet: average $J(^{13}\text{C}-^{31}\text{P}) = 5$ Hz. ^d Apparent doublet: average $J(^{13}\text{C}-^{31}\text{P}) = 10$ Hz (**6a**), 11 Hz (**6b**, **6c**). ^e Apparent triplet: average $J(^{13}\text{C}-^{31}\text{P}) = 6$ Hz.

Table 7. ^{31}P and ^{77}Se NMR Spectroscopic Data for **6a–c** in CDCl_3 Solution

	6a	6b	6c
^{31}P	48.5	47.6	46.4 ^a
^{77}Se	522	not recorded	531 ^b

^a $^2J(^{31}\text{P}-^{31}\text{P}) = 38$ Hz. ^b $^2J(^{77}\text{Se}-^{31}\text{P}_{\text{trans}}) = 71$ Hz; $^2J(^{77}\text{Se}-^{31}\text{P}_{\text{cis}}) = 16$ Hz.

Table 8. Yields, Melting Points, and Mass Spectrometric Data for **6a–c**

	6a	6b	6c
yield (%)	8 ^b	6 ^b	7 ^b
melting point (°C)	209–212 (d)	181–183	201–205 (d)
mass spectrometric data ^a			
M^+	744 (100%)	758 (100%)	772 (100%)
$[\text{PdSe}_2(\text{dppe})]^+$	664 (21%)	664 (25%)	664 (61%)

^a Recorded using FAB; figures are for isotopomers containing ^{80}Se , ^{106}Pd . ^b Isolated yields from **4a–c**: ~70%.

performed on simplified models of **3a**, where the phosphine ligands were replaced by PH_3 groups (with no simplification of the diselenolate ligand). More detailed models, with PR_3 groups ($\text{R} = \text{Me}, \text{Et}, \text{Pr}, \text{Bu}$), were also optimized, starting from the experimental **3a** geometry, progressively pruned of the outermost methylene groups in the alkyl chains. Using the Gaussian 98²⁵ suite of programs, calculations were run at the B3LYP/6-31G(d,p) level²⁶ with the LANL2DZ valence functions and effective core potentials²⁷ for the Pd and Se atoms. For the model with $\text{R} = \text{Bu}$, the limited 3-21G basis set^{25,28} was used for atoms of the methyl and adjacent

methylene groups and the 6-31G(d,p) set²⁹ for the other C and H atoms and for the P atoms. Frequency calculations, to check the nature of stationary states, were performed for the models not subject to constraints, and unscaled ZPE corrections were applied when energy comparisons were of interest. Parts of the results were interpreted in the light of natural bond orbital (NBO) analysis procedures.³⁰ For graphics, Molden³¹ was employed. Atomic coordinates for the optimized models are available from the authors on request.

Results and Discussion

Preparation of 3a–c and 4a–c. When a mixture of $[\text{Pd}_2(\text{dba})_3]$, tributylphosphine, and one of the bis(cycloalkeno)-1,4-diselenins **2b** or **2c** is heated to reflux in toluene for 1 h, the solution becomes a deep purple color. To obtain the same transformation using **2a**, higher temperature (reflux in xylene) and longer reaction time are required. By manipulation of the stoichiometry, the product obtained after column chromatography can be either the mononuclear (**3a–c**: P/Pd = 2) or dinuclear (**4a–c**: P/Pd = 1) diselenolene (Scheme 3).

The detailed mechanism of the reaction is unclear. However, on the basis of previous research showing cleavage of the C–Se bond in 1,4-diselenins,¹⁷ we postulate a first step of metal insertion into the heterocyclic ring system, followed by loss of the cycloalkyne (Scheme 4).

The forcing conditions required to obtain the products when bis(cyclohexeno)-1,4-diselenin ($n = 4$) is employed are in accord with the proposed mechanism, as expulsion of a cycloalkyne fragment would be favorable for $n = 6$, cyclooctyne being an isolable species, but not for $n = 4$, the ring strain in cyclohexyne being significantly larger.

We believe that these are the first palladium diselenolenes to have been isolated in both mononuclear and dinuclear forms. Mononuclear palladium diselenolenes containing ancillary ligands such as phosphines appear to be almost unknown in the literature. Apart from compounds prepared in our own laboratory, we are aware of only one other set

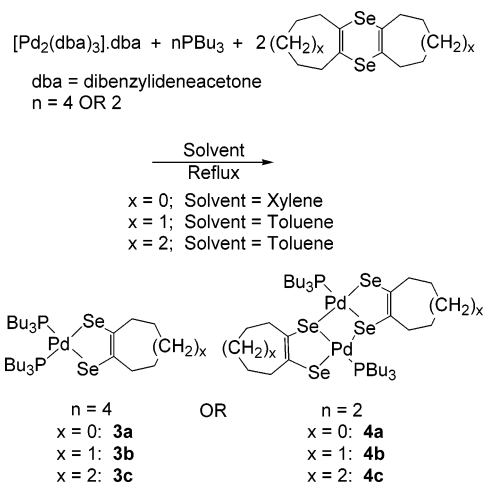
- (22) Altomare, A.; Burla, M. C.; Camalli, M.; Cascarano, G. L.; Giacobuzzo, C.; Guagliardi, A.; Moliterni, A. G. G.; Polidori, G.; Spagna, R. *J. Appl. Crystallogr.* **1999**, *32*, 115.
- (23) Sheldrick, G. M. *SHELXL-93, Program for Crystal Structure Refinement*; University of Göttingen, Göttingen, Germany, 1993.
- (24) (a) Johnson, C. K. *ORTEP—A Fortran Thermal Ellipsoid Plot Program*; Technical Report ORNL-5138, Oak Ridge National Laboratory, Oak Ridge, TN, 1976. (b) Farrugia, L. J. *J. Appl. Cryst.* **1997**, *30*, 565.

- (25) Frisch, J.; Trucks, G. W.; Schlegel, H. B.; Scuseria, G. E.; Robb, M. A.; Cheeseman, J. R.; Zakrzewski, V. G.; Montgomery, J. A., Jr.; Stratmann, R. E.; Burant, J. C.; Dapprich, S.; Millam, J. M.; Daniels, A. D.; Kudin, K. N.; Strain, M. C.; Farkas, O.; Tomasi, J.; Barone, V.; Cossi, M.; Cammi, R.; Mennucci, B.; Pomelli, C.; Adamo, C.; Clifford, S.; Ochterski, J.; Petersson, G. A.; Ayala, P. Y.; Cui, Q.; Morokuma, K.; Malick, D. K.; Rabuck, A. D.; Raghavachari, K.; Foresman, J. B.; Cioslowski, J.; Ortiz, J. V.; Baboul, A. G.; Stefanov, B. B.; Liu, G.; Liashenko, A.; Piskorz, P.; Komaromi, I.; Gomperts, R.; Martin, R. L.; Fox, D. J.; Keith, T.; Al-Laham, M. A.; Peng, C. Y.; Nanayakkara, A.; Gonzalez, C.; Challacombe, M.; Gill, P. M. W.; Johnson, B.; Chen, W.; Wong, M. W.; Andres, J. L.; Gonzalez, C.; Head-Gordon, M.; Replogle, E. S.; Pople, J. A. *Gaussian 98*, revision A.7; Gaussian, Inc.: Pittsburgh, PA, 1998.
- (26) (a) Becke, A. D. *J. Chem. Phys.* **1993**, *98*, 1372. (b) Becke, A. D. *J. Chem. Phys.* **1993**, *98*, 5648. (c) Lee, C.; Yang, W.; Parr, R. G. *Phys. Rev. B* **1988**, *37*, 785.
- (27) Hay, P. J.; Wadt, W. R. *J. Chem. Phys.* **1985**, *82*, 270.
- (28) Ditchfield, R.; Hehre, W. J.; Pople, J. A. *J. Chem. Phys.* **1971**, *54*, 724.
- (29) Binkley, J. S.; Pople, J. A.; Hehre, W. J. *J. Am. Chem. Soc.* **1980**, *102*, 939.
- (30) (a) Glendening, E. D.; Reed, A. E.; Carpenter, J. A.; Weinhold, F. *NBO Version 3.1*; University of Wisconsin: Madison, WI, 1990. (b) Foster, J. P.; Weinhold, F. *J. Am. Chem. Soc.* **1980**, *102*, 7211.
- (31) Schaftenaar, G.; Noordik, J. H. *J. Comput.-Aided Mol. Design* **2000**, *14*, 123.

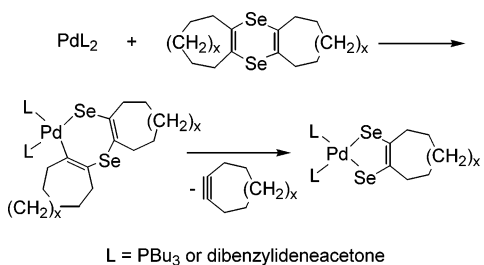
Table 9. Crystallographic Data for Compounds 3a–c

	3a	3b	3c
formula	C ₃₀ H ₆₂ P ₂ PdSe ₂	C ₃₁ H ₆₄ P ₂ PdSe ₂	C ₃₂ H ₆₆ P ₂ PdSe ₂
M _r	749.06	763.08	777.11
crystal system	monoclinic	monoclinic	Monoclinic
space group	P2 ₁ /c (No. 14)	P2 ₁ /c (No. 14)	P2 ₁ /n (alternative setting of No. 14)
a/Å	10.515(2)	10.447(2)	13.210(2)
b/Å	21.196(6)	22.124(4)	22.915(3)
c/Å	16.697(3)	16.772(2)	13.362(3)
β/°	96.65(1)	94.80(1)	105.80(1)
V/Å ³	3696(1)	3863(1)	3892(1)
Z	4	4	4
F(000)	1544	1576	1608
D _c /Mg m ⁻³	1.346	1.312	1.326
crystal size/mm ³	0.15 × 0.40 × 0.50	0.30 × 0.40 × 0.60	0.40 × 0.60 × 0.80
radiation	Mo Kα	Mo Kα	Cu Kα
wavelength/Å	0.71069	0.71069	1.54180
μ/mm ⁻¹	2.574	2.46	6.874
absorption correction	ψ scan	ψ scan	ψ scan
min, max correction factors	0.734, 0.982	0.711, 0.997	0.218, 0.470
data collected	±h, +k, +l	±h, +k, +l	+h, -k, ±l
scan type	ω - 2θ	ω - 2θ	ω - 2θ
2θ range for data/deg	5–54	5–50	7–116
reflections collected	6374	5924	6366
unique reflections	6036	5458	5233
unique observed reflections	2933	2858	4864
with F ₀ > 4σ(F ₀)			
no. of parameters	322	331	341
R1 (observed reflections)	0.0567	0.0538	0.0571
R1 (all reflections)	0.1654	0.1545	0.0598
wR2	0.1456	0.1504	0.1587
goodness of fit	1.005	1.021	1.037
largest features (max, min)	0.609, -0.429	0.471, -0.416	0.880, -1.021
in final ΔF map (e Å ⁻³)			

Scheme 3



Scheme 4



of examples.³² Even the corresponding dithiolenes are rare,³³ although their platinum analogues are well established.³⁴ It is interesting to note here that preliminary examination of the corresponding platinum chemistry has revealed significant

differences in behavior.³⁵ In particular, analogous dinuclear diselenolenes have yet to be isolated. Perhaps the greater lability of palladium complexes is partly responsible for this effect.

Spectroscopic Characterization of 3a–c and 4a–c. The molecular formulas of **3a–c** and **4a–c** have been established by mass spectrometry (Table 4). The mass spectrum of each complex shows an intense cluster corresponding to the molecular ion, with the expected isotope distribution. There is also a major fragment ion formed by the loss of one molecule of tributylphosphine.

The NMR spectroscopic data (Tables 1–3) are in accord with the proposed structures. For the mononuclear species **3a–c**, the two phosphorus atoms are chemically, but not magnetically, equivalent. Analysis of the ⁷⁷Se satellites in the ³¹P NMR spectra allows evaluation of the two different ³¹P–⁷⁷Se coupling constants: ²J(⁷⁷Se–³¹P_{trans}) = 65 Hz (**3a**, **3b**), 67 Hz (**3c**); ²J(⁷⁷Se–³¹P_{cis}) = 16 Hz (**3a–c**). There is also coupling between the two phosphorus nuclei:

- (32) (a) Herberhold, M.; Schmalz, T.; Milius, W.; Wrackmeyer, B. *Z. Naturforsch. B* **2002**, *57*, 53. (b) Herberhold, M.; Schmalz, T.; Milius, W.; Wrackmeyer, B. *Z. Anorg. Allg. Chem.* **2002**, *628*, 979.
- (33) (a) Davison, A.; Edelstein, N.; Holm, R. H.; Maki, A. H. *Inorg. Chem.* **1964**, *3*, 814. (b) Schrauzer, G. N.; Mayweg, V. P. *J. Am. Chem. Soc.* **1965**, *87*, 1483. (c) van Houten, K. A.; Heath, D. C.; Barringer, C. A.; Rheingold, A. L.; Pilato, R. S. *Inorg. Chem.* **1998**, *37*, 4647.
- (34) (a) Johnson, C. E.; Eisenberg, R.; Evans, T. R.; Burberry, M. S. *J. Am. Chem. Soc.* **1983**, *105*, 1795. (b) Bollinger, C. M.; Rauchfuss, T. B. *Inorg. Chem.* **1982**, *21*, 3947. (c) McCullough, R. D.; Belot, J. A.; Seth, J.; Rheingold, A. L.; Yap, G. P. A.; Cowan, D. O. *J. Mater. Chem.* **1995**, *5*, 1581. (d) Giolando, D. M.; Rauchfuss, T. B.; Rheingold, A. L. *Inorg. Chem.* **1987**, *26*, 1636.
- (35) (a) Khanna, P. K.; Morley, C. P. *J. Chem. Res. (S)* **1995**, 64. (b) Webster, C. A.; Morley, C. P. Unpublished observations.

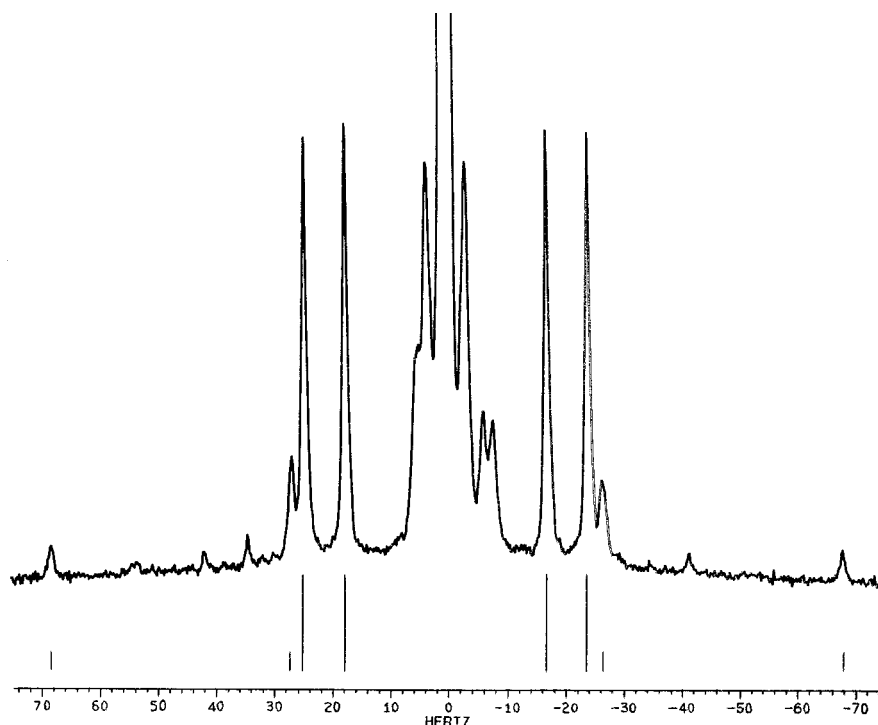


Figure 1. ^{31}P NMR spectrum of **3b**, showing ^{77}Se satellite structure.

$^2J(^{31}\text{P}-^{31}\text{P}) = 44$ Hz (cf. *cis*- $[\text{PdCl}_2(\text{PMe}_3)_2]$, $^2J = 8$ Hz; *cis*- $[\text{PdCl}_2\{\text{P}(\text{OMe})_3\}_2]$, $^2J = 80$ Hz).³⁶ Figure 1 shows the relevant portion of the ^{31}P NMR spectrum of **3c** as an example, with the eight lines resulting from the $^{31}\text{P}-^{77}\text{Se}$ interaction highlighted. The other lines in this spectrum arise from coupling to various ^{13}C nuclei. As expected in these symmetrical molecules there is only one ^{13}C resonance for the olefinic carbon atoms in the alicyclic ring, and only one signal in the ^{77}Se NMR spectrum. As these nuclei constitute the X part of separate AA'X systems, five lines might be expected in each case. In practice, the outer two lines are too weak to be observed, and an apparent triplet is observed, with the separation of the peaks equal to the average coupling constant $^nJ(^{31}\text{P}-\text{X})$ ($\text{X} = ^{13}\text{C}$, $n = 3$ or $\text{X} = ^{77}\text{Se}$, $n = 2$). The ^{77}Se NMR spectrum of **3c** is shown in Figure 2 as an example.

For the dinuclear species **4a-c**, the selenium NMR spectra contain two signals corresponding to the terminal and bridging selenium atoms. The resonance due to the bridging selenium atoms is a doublet of doublets, showing coupling to the *cis* ($^2J = 9$ Hz) and *trans* ($^2J = 110-111$ Hz) phosphorus atoms. These coupling constants are similar to those observed in the analogous triphenylphosphine complexes.¹⁴ The signal corresponding to the terminal selenium atoms is an apparent singlet, as the expected small coupling to the neighboring *cis* phosphorus atoms is not resolved.

The ultraviolet/visible spectra of **3a-c** and **4a-c** are all similar and contain absorption maxima around 560 and 410 nm. The extinction coefficients of these bands are significantly greater (by a factor of more than 10^2) for the dinuclear complexes. For example, for **3c** (10^{-3} mol dm^{-3}

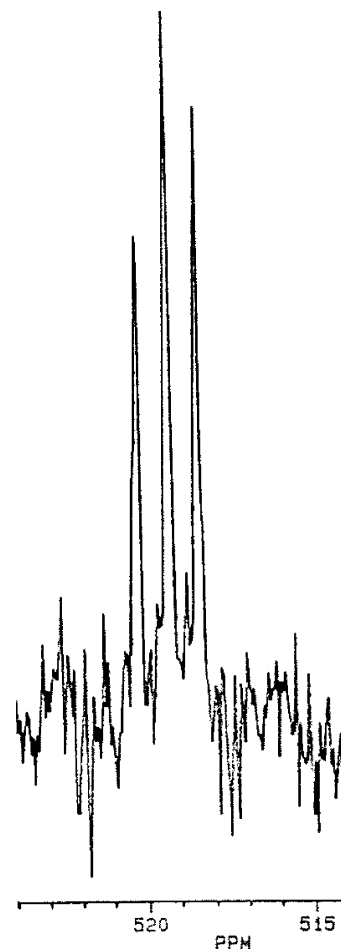


Figure 2. ^{77}Se NMR spectrum of **3b**.

solution in hexane), $\epsilon = 140$ and 420 $\text{dm}^3 \text{mol}^{-1} \text{cm}^{-1}$ at 560 and 410 nm respectively; for **4c** (10^{-4} mol dm^{-3} solution

(36) Berger, S.; Braun, S.; Kalinowski, H. O. *NMR Spectroscopy of the Non-Metallic Elements*; Wiley: London, 1997; p 954.

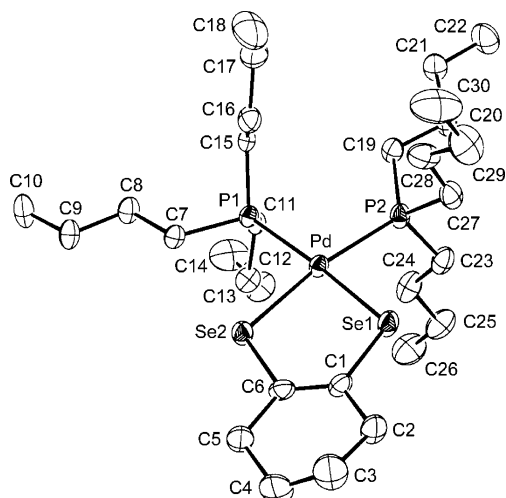


Figure 3. Molecular structure of **3a** with H atoms omitted for clarity. In this and following ORTEP drawings, 20% probability ellipsoids are shown.

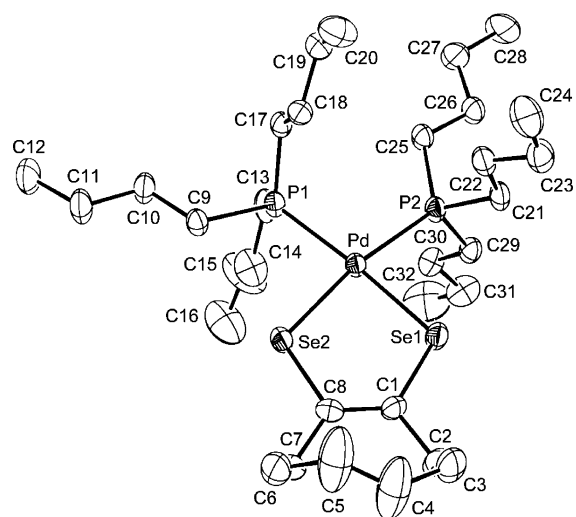


Figure 5. Molecular structure of **3c** with H atoms omitted for clarity.

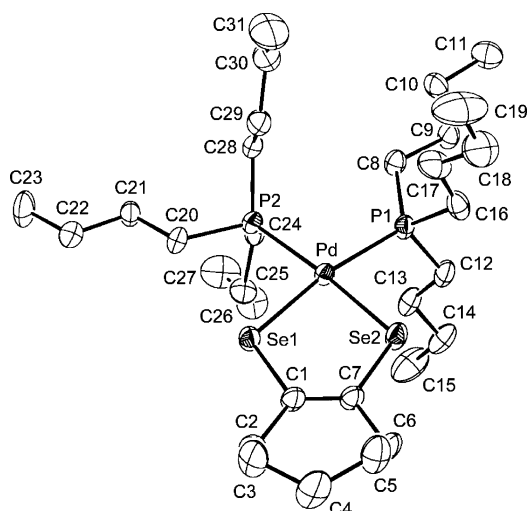


Figure 4. Molecular structure of **3b** with H atoms omitted for clarity.

in hexane), the corresponding values are $\epsilon = 2100$ and $8700 \text{ dm}^3 \text{ mol}^{-1} \text{ cm}^{-1}$. Complexes **4a–c** are deep purple in color, unlike their triphenylphosphine analogues, which are dark green. This is a consequence of a small (25–30 nm) hypsochromic shift in the wavelengths of the two bands in the visible region of the absorption spectra on changing from PPh_3 to PBU_3 , accompanied by an increase in the relative intensity of the higher-wavelength band. We do not believe that these changes reflect significant differences in electronic or molecular structure.

X-ray Structures of 3a–c. The molecular structures of **3a–c**, determined by X-ray structural investigations, are shown in Figures 3–5. Selected bond lengths and angles are listed in Table 10. Each complex consists of a distorted square-planar PdSe_2P_2 core, with only the outer atoms of the hydrocarbon ring and the butyl chains protruding significantly from this plane. The structural parameters for the central portions of the three compounds are very similar. The Pd–Se distances in the three structures, lying in the range 2.396(1)–2.422(1) Å, are shorter than those to the monodentate benzeneselenolate SePh^- in the compounds $[\text{Pd}(\text{SePh})_2(\text{dppe})]$ [2.444(1), 2.480(1) Å]³⁷ and *trans*- $[\text{Pd}$

Table 10. Selected Bond Lengths (Å) and Angles (deg) in the Structures of **3a–c**

	3a	3b	3c
Pd–P(1)	2.325(2)	2.318(3)	2.326(2)
Pd–P(2)	2.319(3)	2.326(3)	2.334(2)
Pd–Se(1)	2.4183(12)	2.402(1)	2.4223(9)
Pd–Se(2)	2.3965(14)	2.419(1)	2.4034(8)
Se(1)–C(1)	1.887(10)	1.90(1)	1.877(7)
Se(2)–C(6)	1.916(9)		
Se(2)–C(7)		1.87(1)	
Se(2)–C(8)			1.900(7)
C(1)–C(6)	1.305(12)		
C(1)–C(7)		1.31(1)	
C(1)–C(8)			1.345(10)
P(2)–Pd–P(1)	99.78(9)	100.2(1)	99.58(6)
P(1)–Pd–Se(2)	88.68(7)	84.34(7)	88.52(4)
Se(2)–Pd–Se(1)	87.07(4)	86.66(4)	86.69(3)
Se(1)–Pd–P(2)	84.60(7)	88.81(8)	85.28(5)
Pd–Se(1)–C(1)	104.3(3)	104.2(4)	104.8(2)
Se(1)–C(1)–C(6)	122.9(7)		
Se(1)–C(1)–C(7)		122.4(8)	
Se(1)–C(1)–C(8)			122.3(5)
C(1)–C(6)–Se(2)	120.9(8)		
C(1)–C(7)–Se(2)		121.7(8)	
C(1)–C(8)–Se(2)			120.4(5)
C(6)–Se(2)–Pd	104.8(3)		
C(7)–Se(2)–Pd		105.0(3)	
C(8)–Se(2)–Pd			105.4(2)

$(\text{SePh})_2(\text{PBU}_3)_2]$ [2.4609(4) Å]³⁸; they are also shorter than the distances to the SeCN^- anion in the compounds $[\text{Pd}(\text{SeCN})_2(\text{dppe})]$ [2.477(1) Å]³⁹ and $[\text{Pd}(\text{SeCN})_2(\text{dppp})]$ [2.458(1), 2.488(1) Å].³⁹ On the other hand, the present Pd–Se distances are comparable to those [mean values 2.406(7), 2.407(1), 2.4022(5), and 2.4023(7) Å, respectively] to the structurally related bidentate ligands in the diselenolenes $[\text{NMe}_4][\text{Pd}(\text{C}_3\text{S}_3\text{Se}_2)_2]$,⁴⁰ $[\text{NBU}_4][\text{Pd}(\text{C}_3\text{S}_3\text{Se}_2)(\text{Se}_2\text{CNEt}_2)]$,⁴¹

(37) Singhal, A.; Jain, V. K.; Varghese, B.; Tiekink, E. R. T. *Inorg. Chim. Acta* **1999**, *285*, 190.

(38) Alyea, E. C.; Ferguson, G.; Kannan S. *Polyhedron* **1998**, *17*, 2231.

(39) Grygon, C. A.; Fultz, W. C.; Rheingold, A. L.; Burmeister, J. L. *Inorg. Chim. Acta* **1988**, *144*, 31.

(40) Faulmann, C.; Legros, J. P.; Cassoux, P.; Cornelissen, J.; Brossard, L.; Inokuchi, M.; Tajima H.; Tokumoto M. *J. Chem. Soc., Dalton Trans.* **1994**, 249.

(41) Olk, R.-M.; Dietzsch, W.; Kahlmeier, J.; Jorchel, P.; Kirmse, R.; Sieler, J. *Inorg. Chim. Acta* **1997**, *254*, 375.

[K(2.2.2-crypt)]₂[Pd{Se₂C₂(CN)₂}]⁴² and [PPh₄]₂[Pd{Se₂C₂(CO₂Me)₂}]⁴³. Smaller values of Pd–Se distances [mean 2.379(5) Å] in the structure of the similarly related compound [NBu₄]₂[Pd(C₃S₅)(C₃Se₅)]⁴⁴ are likely caused by S/Se disorder. The values of the Pd–P distances in **3a–c**, all in the 2.318(3)–2.334(2) Å range, substantially agree with that [2.333(1) Å] measured for the centrosymmetric *trans*-[Pd(SePh)₂(PBu₃)₂] complex.³⁸ The Se–Pd–Se bond angles in **3a–c** [mean 86.8(2)°] are smaller than those formed by the above pairs of monodentate ligands [99.11(4)°,³⁷ 91.2(1)°, and 94.1(1)°³⁹], and they are also smaller than those formed by the bidentate ones [90.74(9)° and 91.18(9)°,⁴⁰ 93.14(4)°,⁴¹ 91.61(2)°,⁴² 90.03(2)°,⁴³ 91.5(1)°⁴⁴]. This might be ascribed both to geometric requirements of the diselenolene ligands and to steric repulsions between them and the large adjacent trialkylphosphine ligands in the present structures (see below). The coordination geometry in each of the complexes **3a–c** is slightly asymmetric. One Pd–Se bond is ca. 0.02 Å longer than the other, and one P–Pd–Se angle is significantly expanded [mean 88.7(1)° vs 84.7(5)°]. We have previously observed a similar distortion in the structures of palladium and platinum dithiolenes.⁴⁵ It is clear from the NMR data, however, that the asymmetry is not maintained in solution

Computational Studies. Quantum mechanical calculations were undertaken, by the procedures described in the Experimental Section, in an attempt to rationalize some of the unusual structural features noted above and to achieve a better understanding of the bonding in mononuclear diselenolenes and related complexes. A simplified model for **3a** was used initially, with PH₃ groups replacing the tertiary phosphine ligands. Despite the simplification, the model was found to reproduce the experimental geometry with reasonable accuracy, yielding a P–Pd–P angle of 98.4° (vs the experimental value of 99.8°) and an Se–Pd–Se angle of 86.9° (vs 87.1°), although it suffered from a well-known limitation of computational approaches of this type, in producing longer metal–donor atom distances than expected (by 0.04 Å for Pd–P and as much as 0.08 Å for Pd–Se). The values of the Se–C and C–C distances from the calculations were also slightly larger than the experimental ones, but this could be ascribed to apparent shortening of the latter distances as a result of thermal motion. The fair agreement obtained in the value of the Se–Pd–Se angle, despite the larger Pd–Se bond lengths from the calculations, was due to an Se···Se separation predicted to be moderately greater (3.427 Å) than that found experimentally [3.316(2) Å].

These preliminary results showed that (a) in the absence of interligand crowding, the system adopts a “symmetrical” geometry, with identical P–Pd–Se angles, and (b) the large

Table 11. Values of Selected Interatomic Distances (Å) and Bond Angles (deg) for Models with Phosphines of Increasing Complexity, Compared with Experimental Data for **3a**^a

	3a	R = Me	R = Et	R = Pr	R = Bu
Pd–Se1	2.418	2.522	2.525	2.527	2.527
Pd–Se2	2.396	2.509	2.514	2.515	2.515
Pd–P1	2.325	2.375	2.396	2.397	2.394
Pd–P2	2.319	2.390	2.407	2.408	2.408
P1–Pd–Se2	88.7	88.4	88.8	88.7	89.0
P2–Pd–Se1	84.6	85.3	84.7	84.9	84.7
P1–Pd–P2	99.8	100.3	100.9	100.9	100.7
Se1–Pd–Se2	87.1	86.0	85.6	85.6	85.6
Se···Se	3.316	3.431	3.424	3.424	3.427

^aLabels as in Figure 6, where conformer geometries for R = Me are shown.

P–Pd–P angle in **3a–c**, primarily imposed by the bulky phosphines (see below), is nevertheless consistent with any requirements that might be set by the diselenolene co-ligand, particularly through its bite size and the consequent preferential use of specific metal orbitals.

The simplified model above was used for a set of geometry optimizations in which the P–Pd–P angle was fixed at the 99.8° experimental value, while the adjacent P–Pd–Se angle was varied in steps (but fixed in the course of each optimization). These calculations confirmed that the minimum-energy conformation indeed exhibits symmetrical geometry, but showed that the bending deformation was not energetically demanding: a geometry with ca. 4° difference in the values of the opposite P–Pd–Se angles, approximately corresponding to the experimental arrangement, lay only 0.14 kcal mol^{−1} above the energy of the symmetrical model, and a 10° difference in the angles merely involved an increase in energy of 1.2 kcal mol^{−1}.

Calculations on more realistic models, with tertiary phosphines PR₃ (R = Me, Et, Pr, Bu) arranged, at the beginning of the optimizations, as the PBu₃ groups in **3a**, yielded in all cases the same type of distortion of the metal environment as found experimentally (Table 11), suggesting that these structural features result from interactions between the innermost parts of the alkyl groups and the selenium atoms. Indeed, with the orientation of phosphine groups shown in Figure 6a for R = Me, but representative of the situation for all the phosphines considered and corresponding to the “experimental” setting, the two Se atoms are involved in different contact interactions with PR₃ methyl groups (or methylene groups for R ≠ Me), as there are two methyls (or methylene groups) in the proximity of Se1 and only one, but at a shorter distance, near Se2. Applying 60° rotations to the PMe₃ groups about the respective Pd–P axis produced the expected interchange of P–Pd–Se angle values. Moreover, two conformers could be identified with symmetrically oriented PMe₃ groups, and their unconstrained geometries substantially attained C₂ symmetry in the course of the optimizations; these are shown in parts b and c of Figure 6. Their energies are close (within 0.3 kcal mol^{−1}) to that of the “unsymmetrical” conformer of Figure 6a; presumably, a preference for the latter is enhanced under the experimental conditions by the presence of alkyl chains longer than those of the models with trimethylphosphines. The substantial

(42) McLauchlan, C. C.; Robowski, S. D.; Ibers, J. A. *Inorg. Chem.* **2001**, *40*, 1372.

(43) McLauchlan, C. C.; Ibers, J. A. *Acta Crystallogr. C: Cryst. Struct. Commun.* **1999**, *55*, 30.

(44) Matsubayashi, G.; Tanaka, S.; Yokozawa, A. *J. Chem. Soc., Dalton Trans.* **1992**, 1827.

(45) Ford, S.; Lewtas, M. R.; Morley, C. P.; Di Vaira, M. *Eur. J. Inorg. Chem.* **2000**, 933.

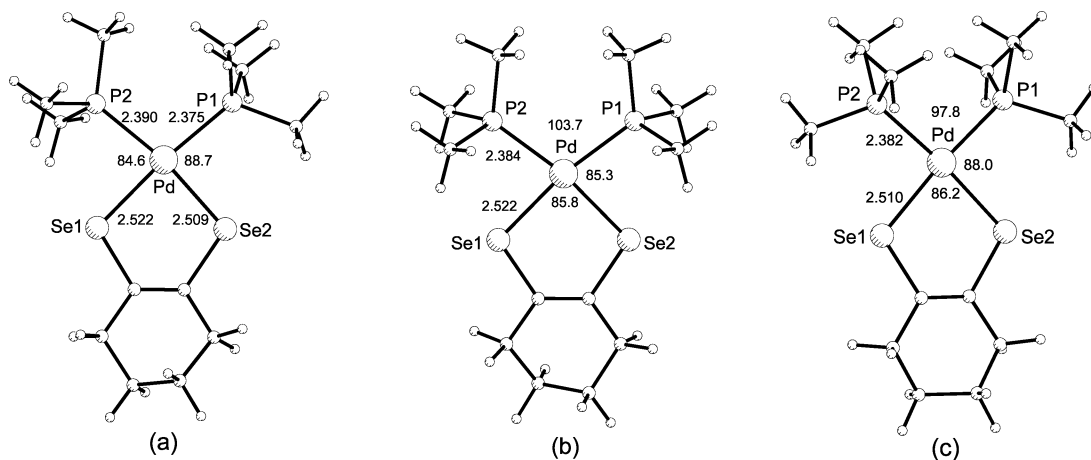


Figure 6. Geometries of conformers of the model system with methylphosphines: (a) unsymmetrical setting (data from column 3 of Table 11); (b, c) symmetrical arrangements, with unique values for Pd–P and Pd–Se distances. Distances are in angstroms, angles in degrees.

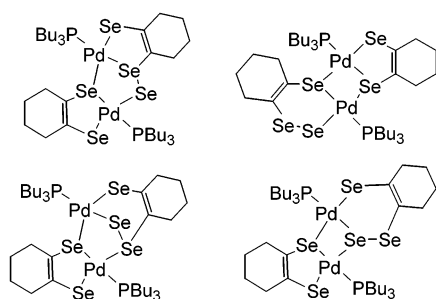
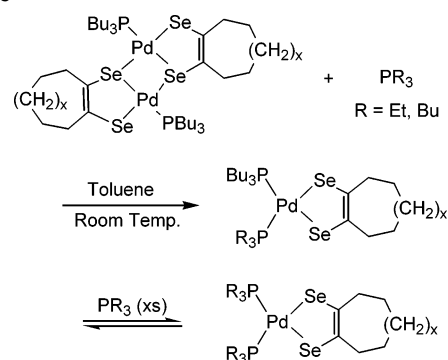


Figure 7. Possible structures of **5a**.

constancy in the value of the P–Pd–P angle for the models of Table 11 indicates, however, that conclusions drawn on the basis of the one with PMe₃ are likely to be general. In particular, the similarity in energies of the conformers of Figure 6a–c and the easy interconversions between them, verified in the course of the calculations, rationalize the time-averaged symmetrization occurring in solution, according to the NMR spectra. More details of the results of calculations on these systems and a discussion of the similarities and differences between factors controlling the geometries of the present diselenolene complexes and those of the previous dithiolene derivatives⁴⁵ are provided with the Supporting Information.

Preparation and Characterization of 5a. In the preparation of **4a**, a second palladium species, **5a**, can be isolated in reasonable yield. Mass spectrometry reveals that this red compound has a formula corresponding to the addition of a selenium atom to the dinuclear diselenolene. The ³¹P NMR spectrum of **5a** contains two singlets, corresponding to two independent, inequivalent tributylphosphine ligands. In the ¹H and ¹³C NMR spectra, there is a corresponding doubling of all resonances for the phosphorus-bound alkyl groups. Similarly, each atom in the two alicyclic rings gives rise to a separate signal. It is clear, therefore, that the C₂ symmetry of **4a** has been lost. Structures for **5a** that are consistent with these observations are shown in Figure 7. Alternatives, such as those incorporating a phosphine selenide ligand, can be excluded on the basis of the NMR spectroscopic data, but distinguishing between the four remaining possibilities has not been possible. Unfortunately, crystals of sufficient quality

Scheme 5



for determination of the structure by X-ray crystallography were not obtained.

Although the mechanism for the formation of **5a** is unknown, we have established that there is no reaction between **4a** and red selenium, which might have been generated by thermal decomposition of the 1,4-diselenin under these conditions. Attempts to prepare compounds analogous to **5a** from **2b** and **2c** were unsuccessful. The reactions with [Pd₂(dba)₃]/PBu₃ lead to **3a,b** and **4a,b** even when conducted in xylene at reflux over extended periods. The addition of red selenium to the reaction mixture also fails to have the desired effect.

Reactions of 4a–c. The only previously reported examples of dinuclear diselenolenes are the triphenylphosphine-palladium complexes prepared in our own laboratory.¹⁴ A difference between these two systems is that no mononuclear product containing triphenylphosphine could be isolated from the reaction of [Pd(PPh₃)₃] with **2a–c**, even though excess phosphine was present in solution. Furthermore the dinuclear complexes **4a–c** do not react with PPh₃, whereas their treatment with excess PBu₃ in toluene solution at room temperature results in rapid cleavage of the Pd–Se–Pd bridge and formation of **3a–c** (Scheme 5). These differences presumably reflect the greater basicity of the trialkylphosphine.

Complexes **4a–c** also react rapidly with an excess of triethylphosphine (Scheme 5). ³¹P NMR spectroscopy shows that the products are not the expected mixed-phosphine

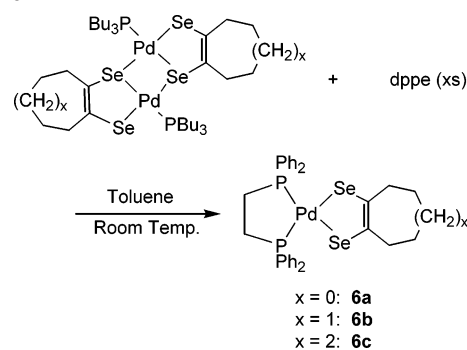
derivatives; instead, there is quantitative conversion to species with triethylphosphine as the only phosphorus-containing ligand. These are presumed to be the mononuclear diselenolenes $[\text{Pd}\{\text{SeC}(\text{R}^1)=\text{C}(\text{R}^2)\text{Se}\}(\text{PEt}_3)_2]$ [$\text{R}^1, \text{R}^2 = (\text{CH}_2)_n$, $n = 4, 5, 6$]. That phosphine exchange takes place in addition to bridge cleavage indicates that the phosphine ligands in these compounds are quite labile. Indeed, under these conditions, it was not possible to isolate the products free of contamination by tributylphosphine complexes.

Mononuclear diselenolenes containing the chelating diphosphine bis(diphenylphosphino)ethane (dppe) can be prepared by the reaction of a mixture of $[\text{Pd}_2(\text{dba})_3]$ and dppe with a bis(cycloalkeno)-1,4-diselenin. The yields of the products **6a–c** are, however, much lower than those of the analogous tributylphosphine complexes **3a–c**. Use of the corresponding 1,2,3-selenadiazole in place of the 1,4-diselenin results in the same species being formed, as the reaction pathway shown in Scheme 1, which leads to azo complexes, does not compete. Nevertheless, the yields of **6a–c** are still poor. This suggests that a key step in the synthesis of diselenolenes by this route involves the formation of an intermediate containing a single monodentate phosphine ligand, a process that is inhibited by the chelate effect in the case of dppe.

Compounds **6a–c** are most efficiently prepared by a ligand-exchange reaction starting with the dinuclear species **4a–c** (Scheme 6). This involves cleavage of the Pd–Se–Pd bridge, accompanied by displacement of the PBu_3 ligand on subsequent ring closure.

The molecular formulas of **6a–c** have been established by mass spectrometry (Table 8). The mass spectrum of each complex shows an intense cluster corresponding to the molecular ion, with the expected isotope distribution. In contrast to the behavior of **3a–c**, loss of the phosphine is not a major fragmentation pathway: the principal fragment ion is formed by elimination of the cycloalkyne from the diselenolene.

Scheme 6



The NMR spectroscopic data (Tables 5–7) are in accord with the proposed structures and resemble those for the analogous tributylphosphine complexes **3a–c**. There are also similarities with the compounds $[\text{M}\{\text{E}_2\text{C}_2(\text{CO}_2\text{Et})_2\}(\text{dppe})]$ ($\text{M} = \text{Pd}, \text{E} = \text{S}; \text{M} = \text{Pt}, \text{E} = \text{S}, \text{Se}$), which we have prepared in a complementary study via addition of activated alkynes to the tetrachalcogenide complexes $[\text{ME}_4(\text{dppe})]$.⁴⁵

Because of the delocalization of the electrons present in the metal–ligand bonding system, diselenolenes, like their sulfur analogues, are expected to display rich and varied chemical behavior. The properties and reactivity of **3a–c**, **4a–c**, and **6a–c** are currently being investigated further.

Acknowledgment. We thank EPSRC for the provision of a research studentship to S.F., Johnson Matthey plc for the loan of palladium salts, and the Ministero dell' Università e della Ricerca Scientifica e Tecnologica for financial support to M.V.

Supporting Information Available: More details and discussion of the results of the computational studies of these systems; crystallographic data in CIF format. This material is available free of charge via the Internet at <http://pubs.acs.org>.

IC040069Y